ELSEVIER

Journal of Molecular Catalysis A: Chemical 162 (2000) 199–207

JOURNAL OF MOLECULAR CATALYSIS A: CHEMICAL

www.elsevier.com/locate/molcata

Redox and catalytic chemistry of Ti in titanosilicate molecular sieves: an EPR investigation

Rajaram Bal, Karuna Chaudhari, D. Srinivas, S. Sivasanker, Paul Ratnasamy *

National Chemical Laboratory, Pune 411008, India

Abstract

An EPR study of Ti^{3+} in titanosilicate molecular sieves, TS-1, TiMCM-41, ETS-10 and ETS-4 is reported. Ti^{4+} is reduced to Ti^{3+} by dry hydrogen above 673 K. Ti ions in TS-1 and TiMCM-41 are located in tetragonally elongated T_d and those of ETS-10 and ETS-4 in a tetragonally compressed O_h geometric positions. Reduction at 873 K revealed the presence of two non-equivalent Ti^{3+} sites in TS-1 and TiMCM-41. Ti^{4+} ions in a tetrahedral geometry are more difficult to reduce than in an octahedral symmetry. The effects of cation exchange and Pt impregnation, on the geometry and reducibility of titanium in ETS-10, are also examined. Interaction of a tetrahedrally coordinated Ti^{3+} with O_2 or H_2O_2 results in a diamagnetic titanium(IV) hydroperoxo species. Under the same conditions, an octahedrally coordinated Ti^{3+} forms a paramagnetic titanium(IV) superoxo species. The higher catalytic activity of TS-1 and TiMCM-41 in selective oxidation reactions is probably a consequence of the formation of the hydroperoxy species on their surface during the catalytic reaction. The presence of Pt in the vicinity of Ti enables the use of H_2 and O_2 (instead of H_2O_2) to generate the active hydroperoxy site. The absence of formation of titanium hydroperoxy species in ETS-4 and ETS-10 is the cause of their inactivity in selective oxidation reactions. © 2000 Elsevier Science B.V. All rights reserved.

Keywords: Titanosilicates; Porous materials; EPR of Ti^{3+}; Catalytic oxidation; Structure–reactivity; Redox behaviour of titanium

1. Introduction

Isomorphous substitution of Ti^{4+} in place of Si^{4+} in silicalite structures results in a new class of molecular sieves known as titanosilicates. These materials have been studied extensively because of their remarkable catalytic activity in selective oxidation of organic compounds with hydrogen peroxide, under mild conditions [1,2]. X-ray diffraction, EXAFS and XANES studies have revealed that titanium can be incorporated in the framework structure of TS-1 to a limit of 2.3 Ti atoms per unit cell, without any TiO_2 phase [3,4]. In the case of ETS-10 and ETS-4, the Si/Ti ratio is about 5 [5]. Titanium adopts a variety of coordination geometries, e.g., tetrahedral or pentacoordination in TS-1, TS-2, Ti-beta and TiMCM-41 [3,4] and octahedral in ETS-10 and ETS-4 [5,6]. Due to the differences in the ionic radii of Ti^{4+} (0.68 Å) and Si^{4+} (0.41 Å), the isomorphous substitution of Ti^{4+} in place of Si^{4+} invariably distorts the geometry around Ti^{4+} from an ideal T_d. XANES studies on TS-1 by Lopez et al. [3], and on ETS-10 by Sankar et al. [6] have confirmed such a distorted geometry for titanium.

* Corresponding author. Tel.: +91-20-5893030; fax: +91-20-5893355.

E-mail address: prs@ems.ncl.res.in (P. Ratnasamy).

1381-1169/00/$ - see front matter © 2000 Elsevier Science B.V. All rights reserved.
PII: S1381-1169(00)00290-9

Characterization of titanium in titanosilicates by electron paramagnetic resonance (EPR) spectroscopy is limited as the most common oxidation state of Ti (Ti^{4+}), is EPR silent. However, an EPR active Ti^{3+} with a $3d^1$ electronic configuration ($S = 1/2$) can be generated by thermo-evacuation, reduction with H_2/CO or by irradiation with γ-/UV-rays [7]. The EPR spectrum of a Ti^{3+} ion is highly sensitive to the molecular symmetry and coordination environment. Thus, EPR spectroscopy can be used (i) to distinguish titanium in different coordination geometries and (ii) to differentiate a substitutional location from an extraframework location. Recently, Kevan et al. [8–11] reported the EPR of Ti^{3+} generated by γ-ray irradiation and CO treatment in silicalites (TS-1 and TiMCM-41) and aluminophosphate molecular sieves (TAPO-5, TAPO-11, TAPO-31 and TAPO-36). Here, we report a comparative EPR study on the coordination geometry, reducibility (in H_2) and reactivity of titanium in silicalite structures TS-1, TiMCM-41, ETS-10 and ETS-4. The study reveals that reduction of Ti^{4+} to Ti^{3+} is more difficult in a tetrahedral geometry (TS-1, TiMCM-41) than in an octahedral geometry (ETS-10 and -4). The influence of cation exchange and Pt impregnation on the reducibility of Ti in ETS-10 is also examined. The correlation between the redox and reported catalytic characteristics of Ti in titanosilicate molecular sieves is discussed.

2. Experimental

2.1. Sample preparation

Titanosilicates TS-1, ETS-4 and ETS-10 were prepared and characterized as per the reported procedures [12–14]. Fumed silica (99%, Sigma), tetramethylammonium silicate (TMA silicate; 10 wt.% silica solution, $TMA/SiO_2 = 0.5$; SACHEM, USA), cetyltrimethylammonium chloride/hydroxide (CTMACl/OH; 17.9 wt.% Cl and 6.7 wt.% OH) prepared in the laboratory by partial exchange of CTMACl (25 wt.% aqueous solution, Aldrich) over an ion exchange resin, tetramethylammonium hydroxide (TMAOH; 99%, Aldrich) and Ti butoxide (Aldrich) were used in the preparation.

In the synthesis of TiMCM-41, the molar composition of the synthesis gel in terms of oxides was as follows:

$$SiO_2{:}0\text{–}0.08TiO_2{:}0.089(CTMA)_2O$$

$$:0.155(TMA)_2O{:}18H_2O.$$

In a typical synthesis, 24.6% solution of CTMACl/OH (16.7 g) was taken in a polypropylene beaker and 2.08 g TMAOH dissolved in 10 g water and 13.6 g TMA silicate were added to it while stirring. The thick gel formed was stirred for 15 min. Fumed silica (3.1 g) was then added slowly in about 10 min to the above mixture under stirring. The stirring was continued for 1 h after complete addition. To this thick slurry, 1.04 g of $Ti(OC_4H_9)_4$ (for $Si/Ti = 25$) in 5–6 g of isopropanol was added. Stirring was continued for 1 h. The pH of the final slurry was maintained at 11.5. The mixture was then transferred to a stainless steel autoclave and heated at 383 K for 5 days. The solid material (TiMCM-41) was filtered, washed with deionized water and dried at 373 K in air. The product was then calcined at 823 K, first, in flowing nitrogen (for 3 h) and then, in flowing air (for 6 h) to remove the organic material.

Cesium-exchanged ETS-10 samples (ETS-10(Cs)) were prepared by reacting ETS-10 with 1 M CsCl solution (20 ml per g of sample) at 353 K for 2 h with constant stirring. This procedure was repeated five times. The solid material was then washed with deionized water till the filtrate was chloride-free. The sample was then calcined at 673 K for 8 h in air.

Platinum-impregnated titanosilicates were prepared by reacting calcined TS-1, TiMCM-41, ETS-10(Cs) and ETS-4 samples with an aqueous solution of tetraamine platinum nitrate at 353 K. The solution was evaporated to dryness. The resultant solid sample was calcined at 673 K for 8 h in air. The amount of platinum impregnated was 0.05 wt.%.

2.2. Characterization

The crystalline phase identification and purity of the calcined titanosilicalite samples were checked by XRD (Rigaku Miniflex) using a nickel-filtered CuKα radiation ($\lambda = 1.5406$ Å, 30 kV, 15 mA) over $2\theta =$

5–50° and scan speed = 4°/min for TS-1, ETS-10 and ETS-4 and over $2\theta = 1.5$–10° and scan speed = 1°/min for Ti-MCM-41. The chemical composition, physical parameters like surface area and pore diameter were determined as described earlier [12–14]. The diffuse reflectance UV–Visible (DRUV–Vis) spectra were measured using a Shimadzu UV-2101 PC spectrophotometer. Fourier transform infrared (FTIR) spectra (400–4000 cm^{-1}) of the samples as Nujol mulls were recorded on a Pye Unicam SP-300 spectrophotometer. EPR spectra of the reduced samples were measured using a Bruker EMX spectrometer operating at X-band frequency and 100 kHz field modulation. The samples were taken in sealed Suprasil quartz tubes (4.5 mm o.d.) for measurements at 77 and 298 K. The spectral simulations were done by using a Simfonia software package.

2.3. Sample treatments

The calcined samples were initially evacuated (10^{-3} Torr) and dehydrated by gradually raising the temperature from 298 K to a set value in about 4–5 h and then kept at that temperature for a further period of 6 h. The samples, thus activated, were treated with a flow of dry hydrogen (20 ml/min) at 523, 673 and 873 K (except for ETS-4 which was reduced only at 523 and 673 K) for 6 h. Then the sample was cooled to 298 K and transferred into EPR tubes. Necessary care was taken to prevent contact with atmospheric oxygen. The integrity of all the structures after reduction with dry hydrogen was confirmed by XRD. The UV–Vis diffuse reflectance spectra of the samples after reduction and subsequent exposure to air was similar to that of the fresh samples confirming the location of Ti in framework positions during the reduction–oxidation processes.

3. Results and discussion

The XRD patterns of the calcined TS-1, TiMCM-41, ETS-4 and ETS-10 samples confirmed their phase purity. No EPR spectrum was observed for all the calcined samples at both 298 and 77 K, suggesting that all titanium ions are present in the +4 oxidation state. Only ETS-4, ETS-10 and, to some extent, TS-1 could be reduced by hydrogen at 673 K. However, all the samples, including Ti-MCM-41, could be reduced (to Ti^{3+}) at 873 K. The XRD patterns of the reduced samples showed no major changes in their structural integrity after reacting with hydrogen.

Fig. 1 shows the EPR spectra of the reduced samples at 77 K. The signals near 3500 G (below $g = 2$) are typical of isolated Ti^{3+} ions. The positions of the Ti^{3+} signals are sensitive to the silicalite structure (Fig. 1). The spectra for TiMCM-41 and ETS-10 show additional signals at $g = 2.021$, 2.008 and 2.002 (indicated by an asterisk " * ") attributable to surface-bound superoxide radical anions, of the type $Ti^{IV}(O_2^-)$ [15]. The spectra obtained after normalization (with respect to the Ti atoms in TS-1) indicate that the overall signal intensity of Ti^{3+} ions decreases in the order ETS-10 > ETS-4 > TS-1 at 673 K and ETS-4 > ETS-10 > TiMCM-41 > TS-1 at

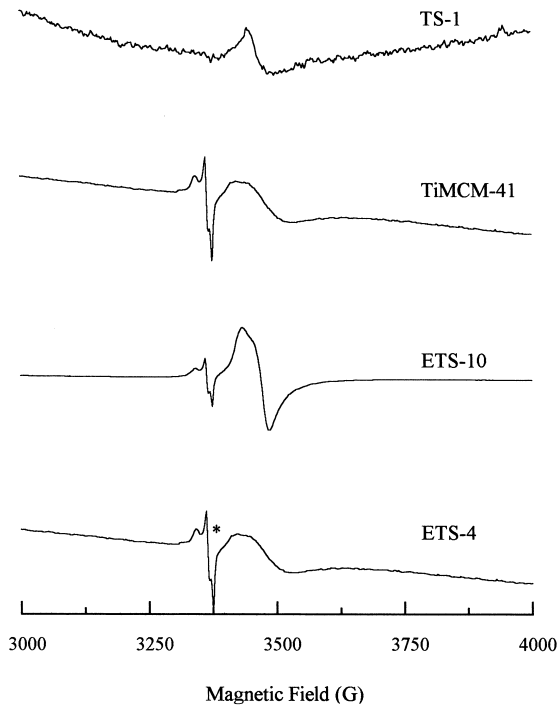

Fig. 1. X-band EPR spectra (at 77 K) of Ti^{3+} in titanosilicate molecular sieves after reduction with dry hydrogen at 873 K for TS-1, TiMCM-41 and ETS-10 and at 673 K for ETS-4 samples. Signals denoted by an asterisk correspond to superoxo radical species.

873 K. Apparently, it is more difficult to reduce Ti in a tetrahedral coordination geometry (as in TiMCM-41 and TS-1) than that in an octahedral geometry (ETS-10 and ETS-4). The spin Hamiltonian parameters of Ti^{3+} ions in the present samples are listed in Table 1. The intensity of the Ti^{3+} signals increased when the reduction was carried out at 873 instead of 673 K. This increase in the signal intensity was 1.9 times for TS-1 and 2.4 times for ETS-10. In the case of ETS-10, $g_{\parallel} > g_{\perp}$ while in the case of ETS-4, $g_{\perp} > g_{\parallel}$ (Table 1). For both TS-1 and TiMCM-41, $g_{\perp} > g_{\parallel}$. The spectra of the TS-1 and TiMCM-41 reduced at 873 K indicated the presence of two non-equivalent Ti^{3+} species (I and II). Both the species have an axial g symmetry in TS-1 ($g_{\parallel} = 1.930$, $g_{\perp} = 1.956$ for species I and $g_{\parallel} = 1.916$, $g_{\perp} = 1.956$ for species II) while in TiMCM-41, species I is characterized by rhombic g values ($g_z = 1.894$, $g_x = 1.938$, $g_y = 1.974$) and species II by axial g values ($g_{\parallel} = 1.902$, $g_{\perp} = 1.958$). Reduction at lower temperatures (673 K) resulted in species I only.

ETS-10 samples were exchanged with Cs^+ ions to examine the interaction of extra-framework ions with titanium. The exchanged samples (ETS-10(Cs)) were then subjected to reduction with hydrogen at 673 K. The spectrum of ETS-10 containing Na^+/K^+ ions (Fig. 2) is characterized by axial g values, with $g_{\parallel} > g_{\perp}$. On exchanging with Cs^+, the spectrum corresponded to a rhombic g tensor with $g_z < g_x$, g_y (Fig. 2). On Cs^+ exchange, the intensity of Ti^{3+} signals decreased by about three times. Platinum (0.05 wt.%)-impregnated ETS-10(Cs) samples showed spectra similar to that of ETS-10(Cs) except that the intensity of the Ti^{3+} signals increased by about 2.4 times compared to the ETS-10(Cs) sample (Fig. 2). While the reduction in Ti^{3+} intensity by Cs is attributed to greater stabilization of Ti^{4+} by the more basic and larger Cs atoms, the increase in intensity by Pt is due to better activation of the reductant molecules (H_2). In other words, both Cs and Pt influence the geometry of the titanium site.

Platinum impregnation in TS-1, TiMCM-41 and ETS-4 also affected their EPR spectra (Fig. 3 and Table 1). The intensity of Ti^{3+} signals was enhanced in the case of both TS-1-Pt (three times) and TiMCM-41-Pt (1.35 times). Thus, as already noted in the case of ETS-10, Pt causes enhanced reduction of Ti^{4+} in TS-1 and TiMCM-41.

The spin Hamiltonian parameters of Ti^{3+} are sensitive to the coordination geometry and the electronic ground state [16]. In a perfect tetrahedral (T_d) or octahedral (O_h) coordination, the spin–lattice relaxation time (T_{1e}) of a $3d^1$ ion is short and the spectra are observable only at very low temperatures (liquid He). However, in the titanosilicalites (especially ETS-4 and ETS-10), Ti^{3+} signals could be observed even at 298 K, suggesting a long spin–lattice relaxation as a consequence of a distorted coordination geometry.

Table 1
EPR spin Hamiltonian parameters of Ti^{3+} in titanosilicate molecular sieves at 77 K

Sample	Reduction temperature (K)	Species	$g_{\parallel}$	$g_{\perp}$	g_z	g_x	g_y
ETS-10	873		1.969	1.942			
	673		1.966	1.941			
ETS-10(Cs)	673				1.869	1.944	1.959
ETS-10(Cs)-Pt	673				1.870	1.943	1.959
ETS-4	673		1.863	1.930			
ETS-4-Pt	673	I	1.870	1.920			
		II	1.863	1.930			
TS-1	873	I	1.930	1.956			
		II	1.916	1.956			
	673	I	1.930	1.956			
TS-1-Pt	673	I	1.931	1.955			
TiMCM-41	873	I	1.902	1.958			
		II			1.894	1.938	1.974
TiMCM-41-Pt	873	I	1.906	1.958			
		II			1.894	1.938	1.974

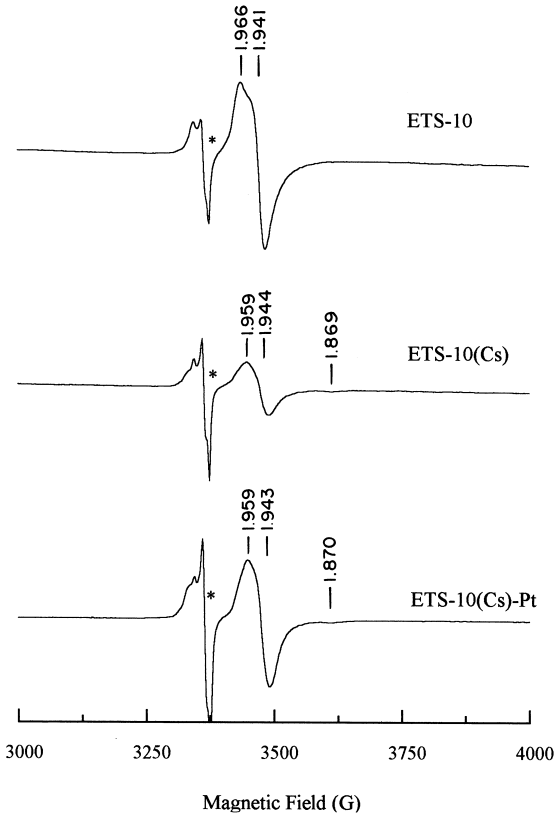

Fig. 2. EPR spectra (at 77 K) showing the influence of Cs exchange and Pt impregnation on the intensity of Ti^{3+} signals in ETS-10 samples reduced in dry hydrogen at 673 K. Signals denoted by an asterisk correspond to superoxo radical species.

Ti^{3+}, with one unpaired electron, has a ^2D ground state. When the ion is subjected to a perfect cubic crystalline field from a tetrahedral or an octahedral coordination, its five-fold orbital degeneracy is lifted into an orbital doublet (^2E) and a triplet (^2T) states. In a tetrahedral coordination, the doublet lies lower in energy, while in an octahedral coordination, the triplet has lower energy. An additional trigonal or tetragonal distortion further lifts the degeneracy of the doublet and triplet levels and results in anisotropic g values. Fig. 4 depicts the d-orbital splitting under the influence of low-symmetry crystal field environments.

In a tetrahedral coordination, if the tetragonal distortion is positive (tetragonal compression), the $d_{3z^2-r^2}$ orbital lies lower in energy. If the distortion is negative (tetragonal elongation), $d_{x^2-y^2}$ is the low-lying orbital. Considering the distortion axis as the *z*-direction, the g values to first order for a tetrahedral coordination are expressed as follows:

$$g_{\parallel} = g_e \text{ and } g_{\perp} = g_e - (6\lambda/\Delta)$$

(tetragonal compression)

$$g_{\parallel} = g_e - (8\lambda/\Delta) \text{ and } g_{\perp} = g_e - (2\lambda/\Delta)$$

(tetragonal elongation).

Here $g_e = 2.0023$, λ is the spin–orbit coupling constant (154 cm^{-1} for Ti^{3+}) and Δ is the energy separation between the degenerate triplet and doublet levels in the cubic tetrahedral field (Fig. 4). Thus, for a tetragonal compression, the g values vary in the order $g_{\perp} < g_{\parallel} \approx g_e$ and for a tetragonal elongation $g_{\parallel} < g_{\perp} < g_e$. The g values presented in Table 1 suggest a tetragonally elongated tetrahedral coordination for titanium in both TS-1 and TiMCM-41.

For Ti^{3+} in an octahedral coordination, the ground state retains some orbital angular momentum even in the zero-order. In this geometry, if the distortion is tetragonal compression, the ground state is the d_{xy} orbital and, if the distortion is tetragonal elongation, the ground state is a degenerate $d_{xz/yz}$ orbital (Fig. 4). In the latter case, Ti^{3+} exhibits a dynamic Jahn–Teller effect and measurements at very low temperatures are required to observe the anisotropic g val-

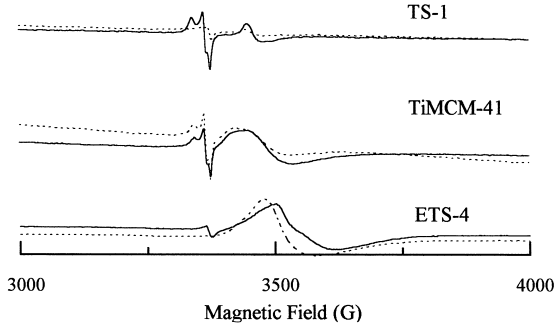

Fig. 3. EPR spectra (at 77 K) revealing the effect Pt impregnation on the intensity of Ti^{3+} signals in titanosilicate molecular sieves reduced in H_2 at 673 K. Dotted curves correspond to samples before Pt impregnation and continuous curves to samples after Pt impregnation.

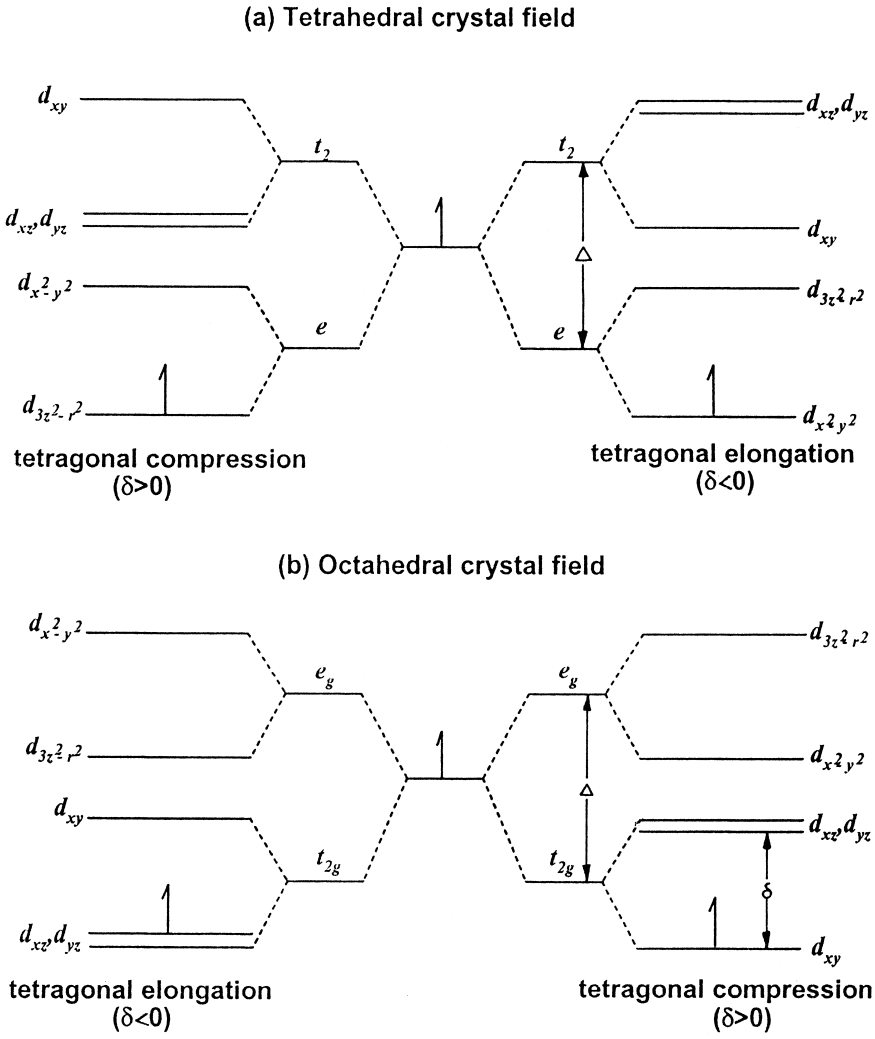

Fig. 4. Splitting of the d-orbitals under the influence of low-symmetry crystal field.

ues. The g value expressions, to first order, for a tetragonally compressed octahedral geometry are:

$g_{\parallel} = g_e - (8\lambda/\Delta)$ and $g_{\perp} = g_e - (2\lambda/\delta)$,

where δ is the energy separation between the d_{xy} and $d_{xz/yz}$ orbitals. Low-symmetry rhombic distortions (D_{2h} site symmetry) results in three g values (g_x, g_y and g_z). The g value expressions for D_{2h} site symmetry are given by:

$g_z = g_e - (8\lambda/\Delta)$, $g_x = g_e - (2\lambda/\delta_x)$,

and $g_y = g_e - (2\lambda/\delta_y)$,

where δ_x and δ_y are the energy separations between d_{xy} and d_{xz} and d_{yz} orbitals, respectively. Although both ETS-10 and ETS-4 possess a tetragonally compressed octahedral geometry, for ETS-10, $g_{\parallel} > g_{\perp}$ while for ETS-4, $g_{\perp} > g_{\parallel}$. This difference can arise from differences in the extent of tetragonal distortion: In the case of ETS-10, the values of Δ and δ are 37,000 and 6120 cm^{-1}, respectively. In contrast, ETS-4 has a lower Δ value of 8800 cm^{-1} and δ equals to 4100 cm^{-1}. In other words, the extent of tetragonal distortion (δ/Δ) is more in the case of ETS-4 than in ETS-10 leading to a reversal of the

relative g values. Cs exchange and Pt impregnation also increase the tetragonal distortion. A UV–Vis band around 700 nm for the reduced ETS-4 sample agrees well with the Δ value estimated from EPR results. In the case of ETS-10, however, the d–d band could not be separated as they overlap with the charge transfer band. In the case of TS-1 and TiMCM-41 samples, the values of Δ fall in the range 12,000–17,100 cm^{-1}.

The stability of the Ti^{3+} ion (against oxidation to Ti^{4+}) in the various titanosilicates was studied by following the intensity of its spectrum after exposure to air (at 298 K) as a function of time. The intensities of the Ti^{3+} signals for ETS-10 and ETS-4 decreased to 50% and 25% of the original value, respectively, in 24 h. In the case of TS-1 and Ti-MCM-41, no Ti^{3+} ion signal could be detected on reduction in H_2 at 673 K. Interestingly, only in the case of ETS-10, an increase in the signal intensity of the superoxide radical anion was observed as a function of time. The variations in signal intensities of Ti^{3+} and superoxide radical anion for ETS-10 after reduction at 673 K and subsequent exposure to air, as a function of time, are shown in Fig. 5. These studies indicate that the stability of Ti^{3+} species (in air) in different titanosilicates varies in the order ETS-10 > ETS-4 > Ti-MCM-41 > TS-1. The instability of Ti^{3+} arises due to its oxidation to Ti^{4+} in the presence of atmospheric oxygen. Depending on the type of the silicate structure and the coordination geometry around titanium, two types of Ti^{4+} species are formed. In the case of structures with titanium in an octahedral geometry (like ETS-4 and ETS-10), one of the Ti–O bonds is broken during the reduction process forming a pentacoordinated Ti^{3+} species. The latter on reoxidation in O_2 forms a $Ti(O_2^-)$ superoxide radical species which is paramagnetic and shows signals at $g_z = 2.021$, $g_y = 2.008$ and $g_x = 2.002$. Fig. 5 showing a decrease in the intensity of Ti^{3+} signals in air and a corresponding increase of $Ti(O_2^-)$ signals as a function of time supports this hypothesis. In samples containing tetrahedral titanium (TS-1, TiMCM-41), during the reduction process, Ti^{3+} ....OH–Si^{4+} type of species are probably formed. The latter readily interacts with molecular oxygen and forms a diamagnetic Ti(IV) hydroperoxo species (Scheme 1). These types of titanium superoxo and hydroperoxo species have been postulated (often without direct experimental evidence) as intermediates in the oxidation of organic substrates by hydrogen peroxide [1,17]. It has also been proposed that the Ti(IV) hydroperoxo species is more reactive than the superoxo species [1,17]. The present studies indicate that the stability and coordination geometry of Ti^{3+} species are important parameters for the reactivity of titanosilicates. The structures with tetrahedral coordination for titanium (TS-1 and TiMCM-41) form titanium hydroperoxo species highly active in selective oxidation reactions while those with octahedral coordination (ETS-4

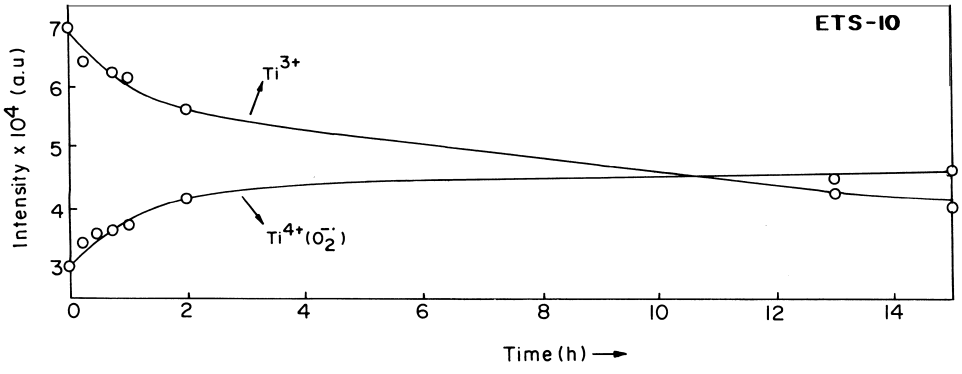

Fig. 5. EPR signal intensity as a function of time of Ti^{3+} and titanium(IV) superoxo species $Ti(O_2^-)$ in reduced ETS-10 samples after exposing to air.

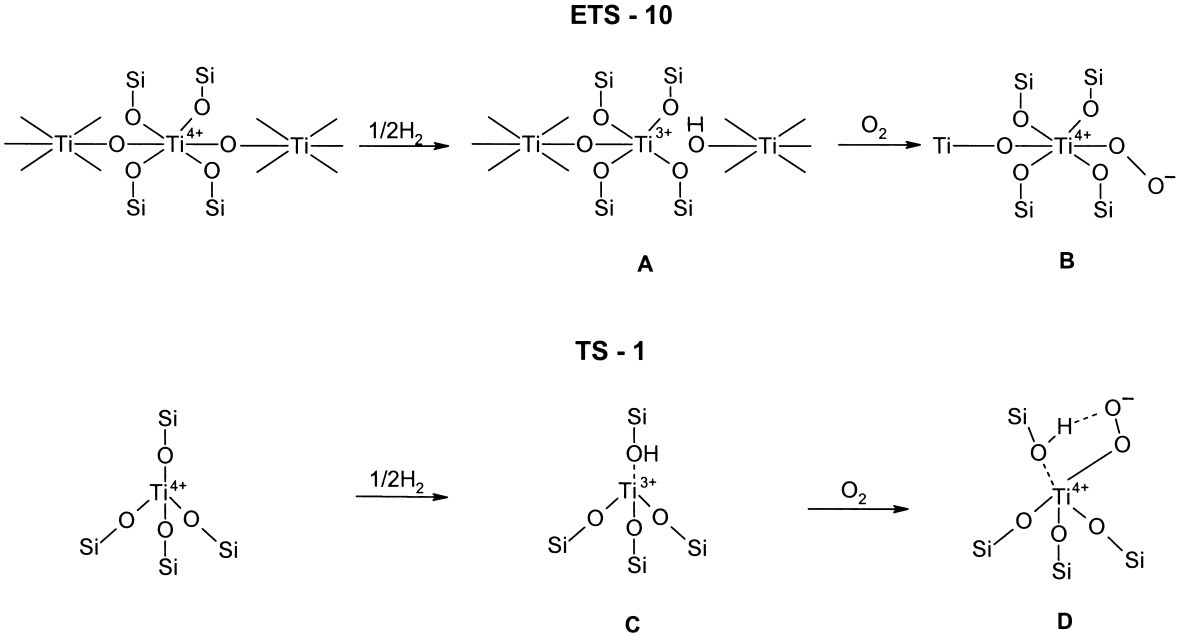

Scheme 1.

and-10) result in a less selective titanium superoxo species.

4. Conclusions

EPR spectroscopy has been used to study the location and local geometry around titanium ions in titanosilicate molecular sieves. Titanium is reduced from +4 to +3 state with dry hydrogen at temperatures above 673 in titanosilicate molecular sieves, TS-1, TiMCM-41, ETS-10, ETS-4. EPR spectra reveal a distorted tetrahedral geometry for titanium in TS-1 and TiMCM-41 and a distorted octahedral geometry for ETS-4 and -10, respectively. The exchangeable cations (in ETS-10 and -4) interact with titanium and influence the local geometry around Ti ions and hence, their energy levels. Platinum impregnation enhances the reducibility of titanium in TS-1 and TiMCM-41. On reduction in H_2 and subsequent oxidation in O_2 of titanosilicate molecular sieves, two types of oxotitanium species of relevance to their catalytic chemistry have been identified; the first is a hydroperoxo titanium species (Ti^{4+}–O–O–H) formed over TS-1 and TiMCM-41; the second is a titanium superoxo species (Ti^{4+}–O_2^-) formed over ETS-4 and ETS-10. The higher catalytic activity of TS-1 and TiMCM-41 in selective oxidation reactions is probably a consequence of the formation of these hydroperoxy species on their surface during the catalytic reaction. The presence of Pt in the vicinity of Ti enables the use of H_2 and O_2 (instead of H_2O_2) to generate larger amounts of the active hydroperoxy site. The absence of formation of titanium hydroperoxy species on ETS-4 and ETS-10 is the cause of their inactivity in selective oxidation reactions.

Acknowledgements

Authors thanks Mr. S. Banerjee for the help in reduction experiments.

References

[1] N. Vayssilov, Catal. Rev.-Sci. Eng. 39 (1997) 209.
[2] B. Notari, Adv. Catal. 41 (1996) 253.
[3] A. Lopez, M.H. Tuilica, J.L. Guth, L. Delmotte, J.M. Popa, J. Solid State Chem. 102 (1993) 480.

[4] S. Bordiga, S. Coluccia, C. Lamberti, L. Marchese, A. Zecchina, F. Boscherini, F. Buffa, F. Genoni, G. Leofanti, G. Petrini, G. Vlaic, J. Phys. Chem. 98 (1994) 4125.
[5] M.W. Anderson, O. Terasaki, T. Ohsuna, A. Philippou, S.P. Mackay, A. Ferreira, J. Rocha, S. Lidin, Nature 367 (1994) 347.
[6] G. Sankar, R.G. Bell, J.M. Thomas, M.W. Anderson, P.A. Wright, J. Rocha, J. Phys. Chem. 100 (1996) 449.
[7] A. Tuel, J. Diab, P. Gelin, M. Dufaux, J.-F. Dutel, Y. Ben Taarit, J. Mol. Catal. 63 (1990) 95.
[8] A.M. Prakash, L. Kevan, J. Catal. 178 (1998) 588.
[9] A.M. Prakash, V. Kurshev, L. Kevan, J. Phys. Chem. B 101 (1997) 9794.
[10] A.M. Prakash, H.M. Sung-Suh, L. Kevan, J. Phys. Chem. B 102 (1998) 857.
[11] A.M. Prakash, L. Kevan, M.H. Zahedi Niaki, S. Kaliaguini, J. Phys. Chem. B 103 (1999) 831.
[12] A. Thangaraj, R. Kumar, S.P. Mirajkar, P. Ratnasamy, J. Catal. 130 (1991) 1.
[13] T.K. Das, A.J. Chandwadkar, S. Sivasanker, J. Chem. Soc., Chem. Commun. (1996) 1105.
[14] A. Philippou, M.W. Anderson, Zeolites 16 (1996) 98.
[15] M. Anpo, M. Che, B. Fubini, E. Farrone, E. Giamello, M.C. Paganini, Top. Catal. 8 (1999) 189.
[16] J.A. Weil, J.R. Bolton, J.E. Wertz, Electron Paramagnetic Resonance: Elementary Theory and Practical Applications, Wiley, New York, 1994, p. 213, Chap. 8.
[17] A.V. Ramaswamy, S. Sivasanker, Catal. Lett. 22 (1993) 239.